Available online at www.sciencedirect.com

ScienceDirect

Physics Procedia 83 (2016) 1424 – 1434

Physics Procedia

9th International Conference on Photonic Technologies - LANE 2016

Absorptivity measurements and heat source modeling to simulate laser cladding

Florian Wirth[a,*], Daniel Eisenbarth[a], Konrad Wegener[b]

[a]inspire AG, ETH Zürich, Technoparkstrasse 1, 8005 Zurich, Switzerland
[b]Institute of Machine Tools and Manufacturing, ETH Zürich, Leonhardstrasse 21, 8092, Zurich, Switzerland

Abstract

The laser cladding process gains importance, as it does not only allow the application of surface coatings, but also additive manufacturing of three-dimensional parts. In both cases, process simulation can contribute to process optimization. Heat source modeling is one of the main issues for an accurate model and simulation of the laser cladding process. While the laser beam intensity distribution is readily known, the other two main effects on the process' heat input are non-trivial. Namely the measurement of the absorptivity of the applied materials as well as the powder attenuation. Therefore, calorimetry measurements were carried out. The measurement method and the measurement results for laser cladding of Stellite® 6 on structural steel S 235 and for the processing of Inconel® 625 are presented both using a CO_2 laser as well as a high power diode laser (HPDL). Additionally, a heat source model is deduced.

Peer-review under responsibility of the Bayerisches Laserzentrum GmbH

Keywords: Laser cladding; direct metal deposition; additive manufacturing; absorptivity; powder attenuation

1. Introduction

The relevance of additive manufacturing technologies is becoming more prevalent, since they enable the manufacturing of complex parts that can hardly be produced by conventional technologies. Laser cladding is among one of these additive manufacturing technologies. It is also known as direct metal deposition (DMD), laser metal deposition (LMD), laser engineered net shaping (LENS), laser additive manufacturing (LAM) or direct energy

* Corresponding author. Tel.: +41-44-633-78-74 ; fax: +41-44-632-11-59 .
E-mail address: wirth@inspire.ethz.ch

Peer-review under responsibility of the Bayerisches Laserzentrum GmbH
doi:10.1016/j.phpro.2016.08.148

deposition (DED). Here, the laser beam creates a melt pool on a substrate material, into which the material to be deposited is blown as a powder, as shown in Fig. 1. Moving the laser beam together with the powder nozzle forward, a single weld track is deposited. Multiple overlapping weld tracks create a layer while multiple layers or single weld tracks one over another can build a 3D structure.

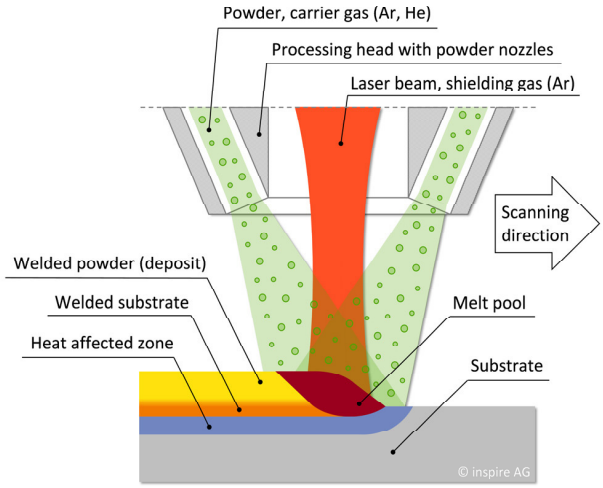

Fig. 1. Principle of laser cladding process.

Laser cladding was developed in the beginning of the 1980s and is widely implemented in industry. Initially, the main application was to repair or correct high-value parts such as tools and dies, as well as turbine and engine components. Owing to high production costs compared to other coating technologies, laser cladding against corrosion and wear was only applied to specialized parts and small lots, for example, for oil drilling or ship diesel engine components (Weisheit et al. 2013). Meanwhile, the application field of laser cladding has increased manifold, especially 3D additive manufacturing and with it, a decrease in production costs. This development can be supported by simulation, if the models have enough predictive capability.

The validity of a process simulation model depends highly on the heat source model. This implies that the local distribution of the heat input and the amount of heat introduced into the interaction zone have to be known. For this, the absorption coefficients of the irradiated materials, the laser beam's intensity distribution and the powder attenuation have to be known. In this paper, a general heat source model is derived followed by experimental measurements, which deliver the data needed in the heat source model.

Nomenclature

C	heat capacity
$I(x,y,z)$	laser beam intensity distribution
k	clad condition parameter
$\dot{m}$	powder feed rate
P_L	laser power
P_L'	transmitted laser power
Q_L	laser heat source
Q_P	powder heat source
s	spot size
x,y,z	coordinates of the Cartesian system
x_p	powder attenuation
α	absorption coefficient
α_e	absorption percentage of the excess powder
α_p	powder absorption coefficient
α_w	workpiece absorption coefficient
α_1	first absorptivity
α_2	second absorptivity
ΔT	temperature difference
Δt	irradiation time
η	overall absorptivity
η_p	powder deposition efficiency
λ	wavelength

2. Heat Source Modeling

The laser beam's interaction with the powder stream and the workpiece surface has already been investigated and modeled by several authors. Marsden et al. (1992) were one of the first to have a closer look at the power absorption during the laser cladding process. According to Marsden et al. (1992) the powder particles in the powder stream attenuate the laser beam directly coming from the laser processing head in the same way as the reflected laser beam. Picasso et al. (1994) included this concept in a simple model, carried out calculations validated by measurements of the powder attenuation and measured the absorption coefficient of the powder as well as the absorption coefficient of the molten clad material for the laser cladding process with an off-axis powder nozzle.

The powder attenuation

$$x_p = \frac{P_L - P_L'}{P_L} \tag{1}$$

is defined as the percentage of the laser power P_L, which is not transmitted through the powder stream and does not reach the workpiece in contrast to the transmitted laser power P_L' that interacts with the workpiece surface like it is indicated in Fig. 2.

The heat source model of Picasso et al. (1994) depends on the workpiece absorption, the powder absorption and the powder attenuation. Meanwhile, there are also more complex models to describe powder attenuation. Recently, Devesse et al. (2015) presented a CFD simulation model of the powder stream, which allows the calculation of the local powder attenuation for each point on the workpiece surface through a ray tracing simulation. Nie et al. (2014) also set up a CFD simulation model of the powder stream in order to simulate the heating of the different powder particles during their flight.

But if there is just an interest in the models' results, it often seems too time-consuming to rebuild the geometrical as well as computational complex models and adapt them to another setup. That is why here a quite simple but yet detailed model is developed which is based on measurement results of material and process properties. Additionally, the following chapter explains the measurement procedure to obtain these results.

One basic idea of the heat source model is that the total laser power can be divided into a usable fraction that contributes to the melt pool heating through workpiece and powder absorption, and a loss fraction that is reflected into the environment by the workpiece as well as by the powder. Fig. 2 breaks down the energy fluxes of the laser cladding process: Initially, the laser power is either transmitted or attenuated by the particles inside the powder jet. The attenuated laser power is absorbed according to the powder absorption coefficient α_p while the complement is reflected out of the process zone. Subsequently, the transmitted laser power is absorbed by the workpiece according to the workpiece absorption coefficient α_w. The laser radiation reflected from the workpiece surface can be divided into three parts. One part is freely reflected out of the process zone and is completely lost. The other two parts interact with the powder particles, where it is assumed, according to Marsden et al. (1992), that such interactions are effectuated analogue to powder attenuation of the initial laser beam. As a result, the second part is also lost, as it is reflected from the powder particles. But the third part is absorbed by the powder particles. The laser radiation absorbed by the powder particles contributes to the melt pool heating if the powder particles hit the melt pool.

In summary, the laser heat source can be given as

$$Q_L = I(x,y,z) \cdot \alpha_w \cdot (1 - x_p) \tag{2}$$

with the laser beam intensity distribution $I(x,y,z)$ in the working plane depending on the coordinates x, y and z. As the powder jet diameter is large compared to the laser beam diameter in the investigated setup, it is assumed that the powder attenuation does not vary within the working plane. In the interaction zone of the laser beam and the powder particles, the flight direction of the particles is approximately parallel to the laser beam. Thus, the heat carried into the melt pool by the powder particles can be expressed as

$$Q_P = I(x,y,z) \cdot (\alpha_p \cdot x_p + \alpha_p \cdot x_p \cdot (1 - \alpha_w) \cdot (1 - x_p)) \cdot k \tag{3}$$

Herein, the clad condition parameter k is a value between 0, indicating that the workpiece surface is not molten, or 1, indicating that the workpiece surface is fully molten with which powder can interact with. Within the melting range, k is interpolated linearly. The values of absorption coefficients and powder attenuation can be found in the results section. In the simulation the workpiece absorption coefficient depends on location and temperature to distinguish between the absorption coefficients of the different materials in different states. Up to the substrate surface level the workpiece absorption coefficient is set to the substrate material absorption coefficient and above to the clad material absorption coefficient. In the melting range the absorption coefficients change linearly between solid and liquid state absorption coefficient. As shielding gas protects the melt pool from oxidation and continuously new powder material is fed into the melt pool, the pure clad material absorption coefficient is associated with the melt.

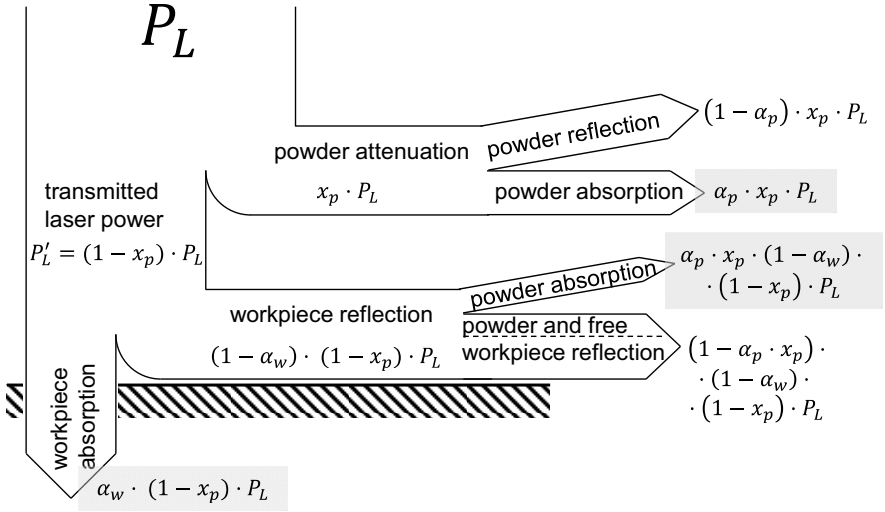

Fig. 2. Breakdown of the energy fluxes within the laser cladding process.

3. Experimental Setup

All measurements were first carried out on a 5-axis CNC laser machine equipped with a 5 kW CO_2 laser (wavelength λ = 10600 nm) and a three-jet powder nozzle. The working distance was 16 mm while the powder focus diameter is approximately 4 mm. Afterwards, some absorption coefficients of the different material surfaces were also measured with a 6 kW high power diode laser (HPDL, λ = 900-1070 nm). The laser processing head was always tilted by 10° to save the optical components from damage by the reflected laser beam. Two different powder materials were investigated, namely MetcoClad® 6 and MetcoClad® 625, which are similar to Stellite® 6 and Inconel® 625 respectively.

According to the attenuation measurements given an off-axis powder nozzle configuration, Picasso et al. (1994) and Marsden et al. (1992) positioned a calorimeter well below the intersection region between the powder and laser beam without any workpiece. This is not possible given a continuous or discrete coaxial powder nozzle configuration. The intersection region length would be a multiple of the working distance since it would not be limited by the workpiece surface. Additionally, the powder would get into the calorimeter. Lin (2000) solved this problem by using compressed air to blow the powder away before reaching the power meter. But with this setup, the interaction length of the powder jet and the laser beam is not clearly defined, whereas it is determined by the working distance during the laser cladding process. Liu et al. (2005) did not protect the power meter, since following impingement, the powder particles are blown away by the carrier gas. The corresponding setup is only possible, if the laser intensity on the power meter surface is low enough, so that there is no thermal damage of the surface and if there is no mechanical damage through the sandblast effect of the powder particles. This can only be achieved by positioning the laser processing head with the powder nozzle far enough away from the power meter. Consequently, the distance is a multiple of the working distance during the laser cladding process.

Herein, an experimental setup for calorimetry measurements is presented which avoids or reduces the aforementioned problems. The calorimeter shown in Fig. 3 was constructed based on Auer (2004) in order to measure the absorptivity of several sample surfaces as well as the powder attenuation and the powder absorption coefficient. The calorimeter consists of a sample holder made of copper, which is surrounded by a styrofoam insulation and a styrofoam lid, which closes the calorimeter after the irradiation time. Three thermocouples inside the sample holder record the temperature, from which the temperature difference ΔT was evaluated using the pulse method, as described by Bergström (2008). The powder catch fixture is only inserted into the calorimeter for measurements where the powder has to be retained inside the calorimeter. Aluminum foil is used to protect the insulation from reflected radiation.

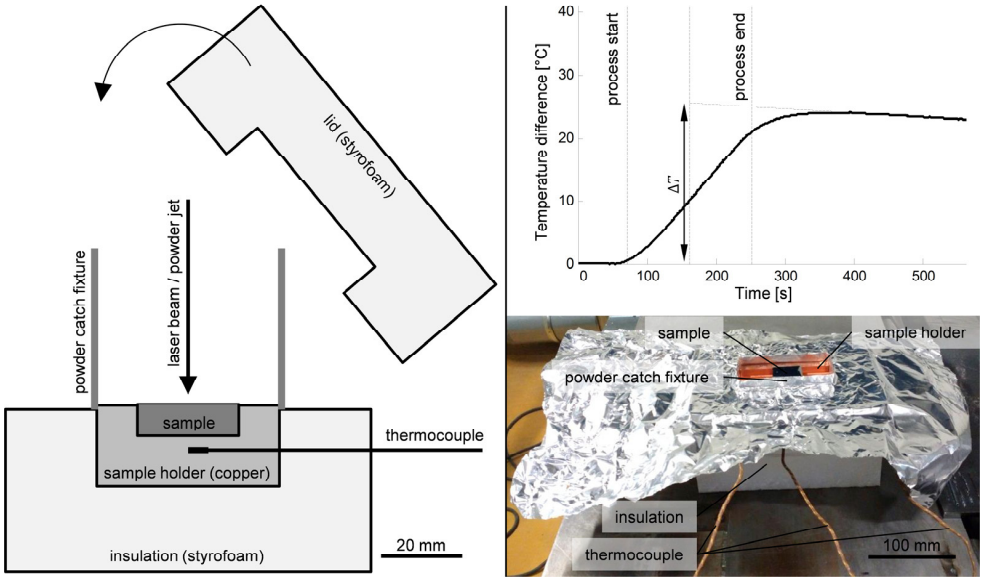

Fig. 3. Cross section of the calorimeter (left), its realization (right below) and a typical temperature profile (right above).

The absorption coefficient

$$\alpha = \frac{\Delta T \cdot C}{P_L \cdot \Delta t} \tag{4}$$

is calculated from the temperature difference ΔT, the laser power P_L, the irradiation time Δt and the temperature dependent heat capacity C of the calorimeter including the sample and powder, which is caught.

Firstly, the absorption coefficients of several materials in the solid and liquid state were measured at the surface using the experimental setup shown in Fig. 3. For measurements at the solid state, the laser beam was defocussed to a spot size of s = 15 mm according to the D86 criterion so that the maximum surface temperature was significantly below the melting temperature. For measurements at the liquid state, the spot size was set to s = 2.5 mm and the laser power was adjusted so that the melt pool diameter was larger than the laser beam diameter, while at the same time no material was evaporated. For all experiments, the shielding and carrier gas flow was set to 3.5 l/min each.

Secondly, the calorimeter was used to measure the powder attenuation and powder absorption coefficient. For these measurements, the laser processing head was moved at a feed rate of 5 m/min over a circular path with a diameter of 15 mm above the sample. The distance of the three-jet powder nozzle to the sample was equal to the working distance. Additionally, the laser power was decreased until the sample surface and the sample absorptivity did not change. When the powder feeder is turned on in this setup, the powder particles fly in the beginning approximately parallel to the laser beam inside the laser-powder interaction zone. After their impingement on the sample surface, the strong gas flow on the sample surface deflects the particles away from the laser beam axis. The strong gas flow stems from the carrier and shielding gas striking the sample surface. So the particles' way out of the interaction zone is short compared to the way inside the interaction zone before the impingement. Hence, the powder attenuation measured on the sample surface only slightly overestimates the real value during the laser cladding process.

For powder attenuation and powder absorption coefficient measurements, three experiments are necessary. In the first experiment, the workpiece absorption coefficient α_w of the sample is measured with zero powder feed rate. In the second experiment, the first experiment is repeated with a defined powder feed rate without the powder catch fixture, so that the powder either directly bounces off the calorimeter after impingement or is blown away by the

carrier and shielding gas. This measurement gives the first absorptivity α_1, which can be used to calculate the powder attenuation

$$x_p = 1 - \frac{\alpha_1}{\alpha_w} \tag{5}$$

In the third experiment, the second experiment is repeated whereby the powder is caught inside the calorimeter. The resulting second absorptivity α_2 can be expressed as

$$\begin{aligned} \alpha_2 &= \frac{\alpha_w \cdot (1-x_p) \cdot P_L + \alpha_p \cdot x_p \cdot P_L + \alpha_p \cdot x_p \cdot (1-\alpha_w) \cdot (1-x_p) \cdot P_L}{P_L} = \\ &= \alpha_w \cdot (1-x_p) + \alpha_p \cdot x_p + \alpha_p \cdot x_p \cdot (1-\alpha_w) \cdot (1-x_p) \end{aligned} \tag{6}$$

Equations (5) and (6) allow the calculation of the powder absorption coefficient

$$\alpha_p = \frac{\alpha_2 - \alpha_1}{\left(1 - \frac{\alpha_1}{\alpha_w}\right) \cdot \left(1 + (1-\alpha_w) \cdot \frac{\alpha_1}{\alpha_w}\right)} \tag{7}$$

It has to be mentioned that the powder catch fixture leads to an increase of the second absorptivity through multiple reflections between the sample, the sample holder, the powder catch fixture and the powder nozzle, if the fixture is too high. In this case, this deviation is determined by comparing the result of an experiment at zero powder feed rate but with the powder catch fixture in place.

4. Results and Discussion

The measured absorption coefficients of the investigated material surfaces are summarized in Fig. 4 as far as they were investigated. “S 235” is a wrought material of standard structural steel. The other surfaces were produced by laser cladding exhibiting different surface quality, namely untreated, polished or ground. It is obvious that the absorption coefficient for the CO_2 laser is always lower than the corresponding one for the HPDL because of the different wavelength. Furthermore the results show that there are materials with a lower absorption coefficient in liquid state than in solid state. This could be observed for example with MetcoClad® 625 in the case of CO_2 laser radiation whereas other materials like S 235 have an opposite behavior. And even for one material such as S 235, the relationship between solid and liquid state absorption coefficient can be inverted when changing the laser type. This can be explained by the fact, that the surface roughness has a different influence on the absorption coefficient depending on the laser wavelength. According to Carpene et al. (2010) the roughness has to be higher than the laser wavelength to increase the absorptivity. This is not given for S 235 as well as polished MetcoClad® 6 under CO_2 laser radiation. When comparing the absorption coefficient of the liquefied untreated surfaces against the corresponding ones of the liquefied polished or ground surfaces, it can be noted that the contaminations from the laser cladding process on the clad surface such as oxides lead to an increase of the absorption coefficient in the case of CO_2 laser radiation. In the solid state, the untreated surfaces’ absorptivity is also higher than the ground or polished surfaces’ absorptivity because of the higher surface roughness. But as soon as the material is molten, the previous surface roughness does not matter anymore, because the surface tension smooths the melt pool surface. This is shown by the two equal measurement results of liquid MetcoClad® 6 under CO_2 laser radiation, where one sample was polished, while the other one was ground. So for liquid surface measurements, it is only important to

remove the contaminations on the clad surface if the original powder material's absorption coefficient shall be measured.

It can be mentioned that the carrier und shielding gas have a negligible influence on the measured absorption coefficients. In general the gas flow cools down a workpiece through forced convection and prevents the emergence of additional heat from oxidation processes. But it was found that the measured absorption coefficient is only 1.3% higher if the gas flow is turned off.

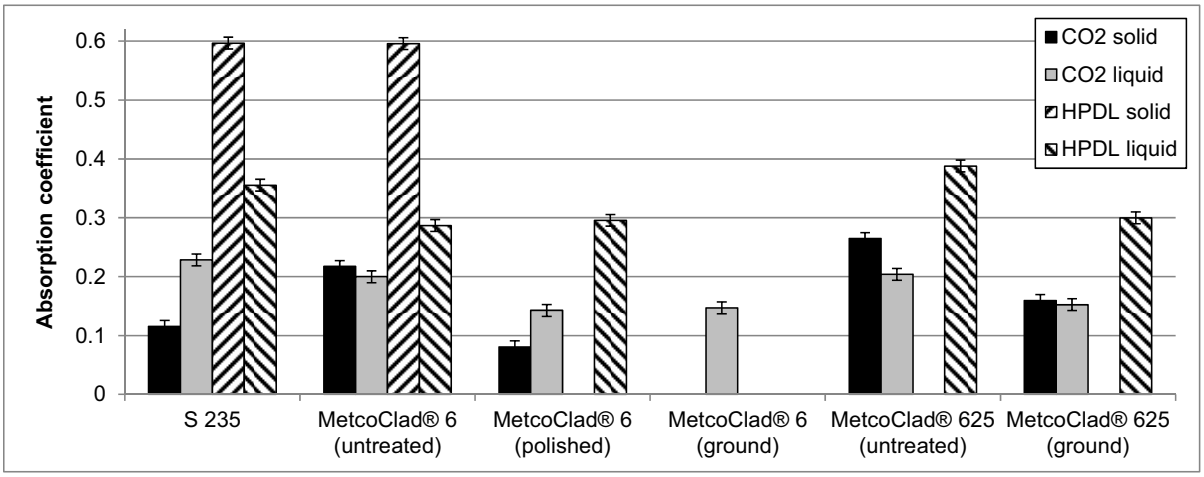

Fig. 4. Absorption coefficients of investigated material surfaces in solid and in liquid state.

The powder attenuation measurements as shown in Fig. 5 (a) demonstrate that there is approximately a linear increase of the powder attenuation with increasing powder feed rate. This has already been demonstrated by Picasso et al. (1994), Frenk et al. (1997) and Liu et al. (2005). The mathematical model of Liu et al. (2005) predicts a declining increase for high powder feed rates. Nevertheless, the presented measurement results as well as the measurements of Liu et al. (2005) do not show this decline yet. Moreover, it is observed that the powder attenuation is higher for a powder with smaller particles because of the higher surface/volume ratio. MetcoClad® 6 shows a particle size distribution with a nominal range of -106 +45 µm according to ASTM B214, while it is -90 +45 µm for MetcoClad® 625.

The powder attenuation was also measured for different laser beam spot sizes. The results in Fig. 5 (b) indicate a decrease of the powder attenuation with increasing spot size. This can be explained with the expansion of the laser beam, whereby more laser radiation can pass the powder jet further away from the laser beam and powder jet axis, where the Gaussian distributed particle density and therefore the powder attenuation are greatest.

These measurement results for the powder attenuation can be linearly approximated as

$$x_p = \frac{\dot{m}}{70\,\mathrm{g/min}} \cdot \left(0.3218 - \frac{0.0545}{\mathrm{mm}} \cdot s \right) \tag{8}$$

for MetcoClad® 6 and

$$x_p = \frac{\dot{m}}{70\,\mathrm{g/min}} \cdot \left(0.5502 - \frac{0.0932}{\mathrm{mm}} \cdot s \right) \tag{9}$$

for MetcoClad® 625 to calculate the powder attenuation x_p to be inserted into equation (3).

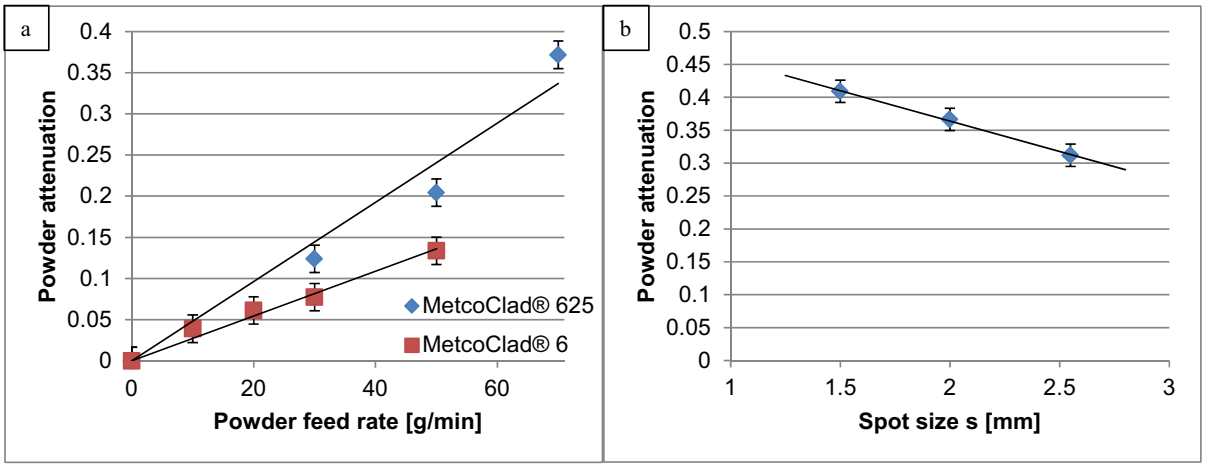

Fig. 5. (a) influence of the powder feed rate on the powder attenuation (CO_2 laser, $\lambda = 10600\ nm$, $s = 2.55\ mm$); (b) influence of the spot size on the powder attenuation (CO_2 laser, $\dot{m} = 70\ g/min$, MetcoClad® 625).

The powder attenuation was also measured using the method presented by Liu et al. (2005) on a machine equipped with a HPDL with a Gaussian intensity distribution and a comparable powder nozzle. There the powder attenuation of MetcoClad® 6 was $x_p = 40\%$ for a spot size $s = 3$ mm and a powder feed rate $\dot{m} = 31$ g/min, while the herein presented method resulted in the powder attenuation $x_p = 8\%$ for an even smaller spot size $s = 2.55$ mm of the CO_2 laser. And the different intensity distribution could only explain a small percentage of the difference in the measured powder attenuation values.

The calculation of the powder absorption coefficient under CO_2 laser radiation gives $\alpha_p = 22\%$ for MetcoClad® 625 and $\alpha_p = 23\%$ for MetcoClad® 6. For the latter, the estimation of Picasso et al. (1994) gives a value in the order of 20%, while Tolochko et al. (2000) measured 25%. Notably, the powder absorption coefficients are in the order of the untreated clad surface absorption coefficients.

Finally, the overall absorptivity η of laser cladding MetcoClad® 6 on S 235 with $P_L = 3080$ W, $s = 2.3$ mm, $\dot{m} = 30$ g/min, feed rate 3.6 m/min and track distance 0.9 mm was measured to be $\eta = 23.4\%$ in case of the CO_2 laser. The overall absorptivity is defined as the ratio of the overall absorbed radiation to the laser power. When the excess powder was retained inside the calorimeter, it was slightly higher $\eta = 25.1\%$. The difference of 1.7% can be explained with a rough estimation which is deduced similarly to equation (3) from the breakdown of the energy fluxes shown in Fig. 2. Accordingly, there is the powder absorption of the primary as well as of the reflected laser beam. Moreover, under the assumption that all powder particles are heated equally, the powder deposition efficiency η_p is equal to the percentage of the powder heat which reaches the melt pool. Hence the absorption percentage of the excess powder

$$\alpha_e = [\alpha_p \cdot x_p + \alpha_p \cdot x_p \cdot (1-\alpha_w) \cdot (1-x_p)] \cdot (1-\eta_p) \tag{10}$$

can be calculated to be $\alpha_e = 1.9\%$, if the absorption coefficients are $\alpha_w = 0.145$ and $\alpha_p = 0.23$, if the powder attenuation is $x_p = 0.0835$ for the used process parameters and if the powder deposition efficiency is $\eta_p = 44\%$. This is a slight overestimation compared to the measured 1.7%. The reason is because powder particles that are blown inside the laser beam, do more probably reach the melt pool. This means that the excess powder consists of particles that are heated below the average.

The measured overall absorptivity of 23.4% is higher than any of the involved single absorption coefficients previously mentioned. This effect is reported by several authors. For instance, Schneider (1998) amounts the overall absorptivity to 30%, while Huang et al. (2008) agree with Hoadley & Rappaz (1992) on 31%. Gedda et al. (2002) even report 39%. This apparent contradiction can be explained by the presented heat source model. According to the model, the laser radiation reflected from the melt pool is partly absorbed by the powder particles. This finding is

confirmed by the observation of Heigel et al. (2016), who noticed a higher laser absorption efficiency of the cladding process with powder in comparison to wire feed. Furthermore, Marsden et al. (1992) detected an increase of the process' overall absorptivity with a rising powder feed rate. This means in applications where the melt pool surface shows a low absorptivity compared to the powder absorption coefficient, process efficiency can be increased by using finer powder material and also by using a powder nozzle creating a smaller powder jet diameter. The latter is confirmed by the simulations of Devesse et al. (2015) for a coaxial powder nozzle with a powder jet diameter of approximately 1.6 mm and a powder feed rate of 2.5 g/min, which are both small in comparison to the herein presented experiments. In these simulations, the small powder jet diameter leads to a local laser beam attenuation of 70% at the laser spot center despite the low powder feed rate.

Finally, the developed heat source model and the measurement results were used for process simulation. The process simulation model takes into account heat transfer, fluid flow, free surface movement and surface tension. Fig. 6 shows that the molten cross sectional area and so the heat input in the simulation agrees with the experimental cross sections. Nevertheless, it has to be mentioned that there are several further factors influencing the cross sectional area like the Marangoni effect. These further factors and process model details will be described in a coming publication.

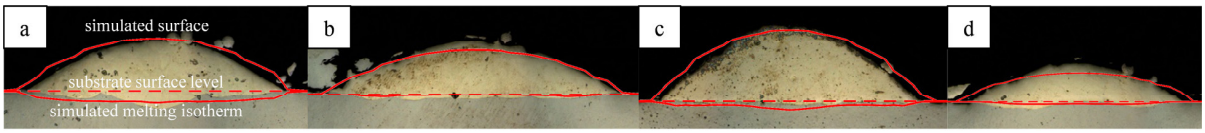

Fig. 6. Comparison of simulated single track cross section contours with experimental cross sections (MetcoClad® 6 on S 235, CO_2 laser, $\lambda = 10600\ nm$, (a, b, c) $P_L = 3415\ W$, (d) $P_L = 2415\ W$, feed rate 3 m/min, (a, b, d) $\dot{m} = 28\ g/min$, (c) $\dot{m} = 39\ g/min$, (a, c, d) $s = 1.9\ mm$, (b) $s = 2.2\ mm$).

5. Conclusion

The presented absorption coefficient measurements show that it is difficult to transfer a laser cladding process from a CO_2 laser source to a HPDL source and vice versa. Especially when the laser beam irradiates the liquid melt pool as well as the solid surrounding, it is not sufficient just to scale the laser power because of the differences in absorption behavior. For example, for S 235, an opposite behavior between the two laser sources was observed when changing from solid to liquid state. Additionally, the intensity distribution of the mentioned laser sources is mostly different. So iterative simulations or experiments are necessary for the process transfer. For the simulation approach, the reported absorption coefficients are necessary input parameters. For the experimental method, the reported absorption coefficients give a useful hint to the needed laser power, if a CO_2 laser shall be replaced by a solid-state laser with different wavelength.

The developed powder attenuation and powder absorption measurement method offers the possibility to characterize the laser powder interaction with little effort, whereas the used calorimeter can also be used to determine the absorption coefficient of different surface states, i.e. solid and liquid. The overestimation of the powder attenuation is smaller than the error of most of other measurement methods like it was indicated for the measurement method presented by Liu et al. (2005). Furthermore, the presented measurement method addresses the real laser cladding process with the powder/gas jet striking the workpiece surface better than other methods with an open jet, because the attenuation is measured directly in the working plane and the workpiece surface widens the powder jet.

Finally, it was demonstrated that the process efficiency can be increased by using finer powder material and a powder nozzle with a smaller powder jet diameter. Moreover, the model results from simulation were compared to experiments indicating the model's capability and potential for future studies.

Acknowledgements

The authors wish to acknowledge the financial support granted by the Swiss Commission for Technology and Innovation (CTI) under grant number 13993.2 as well as the support and advice of the industrial partner Oerlikon Metco, particularly Dr. Thomas Peters and Dr. Arkadi Zikin.

References

Auer, F., 2004. Methode zur Simulation des Laserstrahlschweißens unter Berücksichtigung der Ergebnisse vorangegangener Umformsimulationen. Dissertation TU Munich.

Bergström, D., 2008. The Absorption of Laser Light by Rough Metal Surfaces. Dissertation Luleå University of Technology.

Carpene, E., Höche, D., Schaaf, P., 2010. Fundamentals of Laser-Material Interactions, in "Laser Processing of Materials". In: Schaaf, P. (Ed.). Springer, Heidelberg Dordrecht London New York, pp. 21-47.

Devesse, W., De Baere, D., Guillaume, P., 2015. Modeling of laser beam and powder flow interaction in laser cladding using ray-tracing. Journal of Laser Applications 27, S29208.

Frenk, A., Vandyoussefi, M., Wagniere, J. D., Kurz, W., Zryd, A., 1997. Analysis of the laser-cladding process for stellite on steel. Metallurgical and Materials transactions B 28(3), pp. 501-508.

Gedda, H., Powell, J., Wahlström, G., Li, W. B., Engström, H., Magnusson, C., 2002. Energy redistribution during CO2 laser cladding. Journal of laser applications 14(2), pp. 78-82.

Heigel, J. C., Gouge, M. F., Michaleris, P., Palmer, T. A., 2016. Selection of Powder or Wire Feedstock Material for the Laser Cladding of Inconel® 625. Journal of Materials Processing Technology 231, pp. 357–365.

Hoadley, A. F. A., Rappaz, M., 1992. A thermal model of laser cladding by powder injection. Metallurgical Transactions B 23(5), pp. 631-642.

Huang, Y., Yang, Y., Wei, G., Shi, W., Li, Y., 2008. Boundary coupled dual-equation numerical simulation on mass transfer in the process of laser cladding. Chinese Optics Letters 6(5), pp. 356-360.

Lin, J., 2000. Laser attenuation of the focused powder streams in coaxial laser cladding. Journal of laser applications 12(1), pp. 28-33.

Liu, J., Li, L., Zhang, Y., Xie, X., 2005. Attenuation of laser power of a focused Gaussian beam during interaction between a laser and powder in coaxial laser cladding. Journal of Physics D: Applied Physics 38(10), pp. 1546-1550.

Marsden, C. F., Frenk, A., Wagnière, J.-D., 1992. Power absorption during the laser cladding process, in: "Proc. of the European Conference on Laser Treatment of Materials 1992, Göttingen (ECLAT '92)". In: Mordike B. L.; Bergmann, H. W. (Eds.). DGM Oberursel, pp. 375-380.

Nie, P., Ojo, O. A., Li, Z., 2014. Modeling analysis of laser cladding of a nickel-based superalloy. Surface and Coatings Technology 258, pp. 1048-1059.

Picasso, M., Marsden, C. F., Wagniere, J. D., Frenk, A., Rappaz, M., 1994. A simple but realistic model for laser cladding. Metallurgical and Materials Transactions B 25 (2), pp. 281-291.

Schneider, M., 1998. Laser Cladding with powder: effect of some machining parameters on clad properties. Dissertation University of Twente, Enschede.

Tolochko, N. K., Khlopkov, Y. V., Mozzharov, S. E., Ignatiev, M. B., Laoui, T., Titov, V. I., 2000. Absorptance of powder materials suitable for laser sintering. Rapid Prototyping Journal 6(3), pp. 155-161.

Weisheit, A., Gasser, A., Backes, G., Jambor, T., Pirch, N., Wissenbach, K., 2013. Direct Laser Cladding, Current Status and Future Scope of Application, in "Laser-Assisted Fabrication of Materials". In: Majumdar, J. D., Manna, I. (Eds.). Springer Heidelberg New York Dordrecht London, pp. 221-240.